REGULAR PAPER

Mechanically Active Transducing Element Based on Solid–Liquid Triboelectric Nanogenerator for Self-Powered Sensing

Cong Phat Vo[1] · M. Shahriar[1] · Chau Duy Le[1] · Kyoung Kwan Ahn[2]

Abstract

As power generation from the electronically active materials has been made remarkable progress to scavenge the ambient mechanical energy, harnessing energy from fluidics with liquid–solid contact electrification charging from the flow has become new capabilities to be applied as the sensory module. In this paper, a mechanical fluidic nanogenerator based on solid–liquid contact triboelectrification is demonstrated in which liquid electricity signal can be transferred into from the mechanical motion. This simply designed device is composed of Polytetrafluoroethylene (PTFE) tube and copper electrodes at both ends. To evaluate the effectiveness of the device, deionized water (DI) is poured into the tube and the movement is controlled by air flow from the internal volume difference of the rotating mechanism. The peak current value of the mechanical active transducing element based triboelectric nanogenerator (MAT-TENG) signal is used for analyzing movement speed. Speed gradient was applied for back and forth motion of the liquid column with a stable peak of short circuit current and open circuit voltage was about 0.23 μA and 2.31 V, respectively, at the length of the motion amplitude of 23 mm and frequency of 1 Hz. Finally, the flexible MAT-TENG has shown distinct response with the change of the motion length and speed of the liquid and the results have been achieved with better linearity $\sim R^2 = 0.99$. Therefore, the velocity transducing can be very effective in the practical applications of the TENGs based for self-powered sensing.

Keywords Self-powered · Triboelectric nanogenerator · Solid–liquid triboelectrification · In-plane sliding mode

Abbreviations

TENG	Triboelectric nanogenerator
PTFE	Polytetrafluoroethylene
DI	Deionized
ISC	Short-circuit current
VOC	Open-circuit voltage
FE-SEM	Field-emission Scanning electron microscope
MAT-TENG	Mechanical active transducing element based TENG

✉ Kyoung Kwan Ahn
kkahn@ulsan.ac.kr

1 School of Mechanical Engineering, Graduate School, University of Ulsan, 93, Daehak-ro, Nam-gu, Ulsan 44610, Republic of Korea

2 School of Mechanical Engineering, University of Ulsan, 93, Daehak-ro, Nam-gu, Ulsan 44610, Republic of Korea

1 Introduction

Since last few decades, plenty of monitoring sensors which was used to observe different parameters of structures and machinery have been investigated continuously. Specifically, motion sensors, which can measure the displacement, speed, acceleration, direction, and other motion-related parameters have played an important role in numerous applications, for instance, autonomous vehicles, complex mechanical structure, smart phones, and many other fields. With the technological advancement, nowadays, the sensors can be integrated inside the structure, and as such, it is very important for these sensors to be able to operate independently, sustainably and maintenance-free. Therefore, the ability of the sensors to execute without the external power supply compared to the conventional sensors becomes essential. This kind of sensor shows excellent sensitivity to certain mechanical motions and high efficiency in comparison to the other sensor devices [1–3]. In addition, some of them can measure several characteristics at the same time, namely acceleration [4, 5], pressures [6], direction [7, 8] and so on. Moreover, such sensors can thoroughly utilize all kinds of

abundant and available mechanical energy sources, in our daily life or in natural environment [9, 10], for instance, vibrations [11], human body motions [12, 13], eye-motion [14] and so on.

Self-powered sensor is originated from the changes in the output signals of TENGs based on the basic combination of contact electrification and electrostatic induction [15, 16]. Capturing the electrostatic charges created on the surfaces of two disparate materials when they are brought into physical contact, the contact-induced triboelectric charges can generate a potential difference when the two surfaces are separated by mechanical force, which can drive electrons to flow between the two electrodes. The fundamental working modes of TENG have been reported in the previous work [3] including vertical contact-separation mode, lateral sliding mode, single-electrode mode, free-standing mode. Furthermore, various prototypes of TENGs based on the solid–solid frictions were reported [15, 17–20]. The charges created through friction were closely dependent on the difference of ability to gain or lose electrons after the friction process [17]. Moreover, in each specific applications, various relating materials were modulated or fabricated to further adjust the surface electrostatic charges [3, 15, 17, 18, 21, 22]. However, the result of the output value of the solid–solid TENG could be sensitive to environmental factors, such as temperature, humidity, physical contact [23]. Concerning this, the recent studies on TENGs based on the contact electrification at the liquid–solid interface could mostly solve these problems [24].

Generally, in a liquid–solid TENG, the liquid with changeable shapes usually works as a positive triboelectric material to provide full contact with the solid friction layer to generate more electrostatic charges for a higher output performance [25–27]. Besides, the friction between the solid tribo-layer and the liquid that can make them become a lubricant for contact, resulting in good wear resistance [28–30]. More importantly, the liquid–solid triboelectrification is insensitive to air humidity but the output has a higher sensitivity value than the solid–solid TENGs, which can be used to fabricate more reliable and stable TENGs and TENG based sensors [31]. A few developed working modes of liquid-based TENGs are contact–separation [26, 32] and rotational type [33].

As mentioned, most of the solid–solid TENG is complicated to fabricate and subjected to repeated wear and tear of the tribo-surface due to the continuous rubbing process. The solid–liquid TENGs facilitate from the above discrepancy and ensure long term stability and reliability of the polymer surface. Consequently, a simple and flexible solid–liquid contact triboelectrification based sensors for self-powered mechanical motion detection are rarely reported. In the previous researches [37], the acceleration sensor was designed but safety should be considered when using mercury. In

addition, numerous articles [4–6, 29, 38] also present various types of sensors as listed above, but speed sensors are still relatively rare.

In this study, we fabricated herein a MAT-TENG based on the interaction of the nanostructured PTFE tube with covered copper (Cu) electrodes outside. Besides, the rotary mechanism was also assembled exclusively to inspect its capabilities. When the rotary actuator is applied to the reference displacement lead to the water slides back and forth by airflow inside the tube. The main goal to develop the self-powered sensor utilizing the solid–liquid triboelectrification is to replace the conventional sensor with inexpensive, better flexibility and easy to fabricate approach. The simple construction of the as proposed device can facilitate the easy replacement of the device. Moreover, the liquid movement is spontaneous and instant with respect to the variation of the measurable parameters of the machinery that ensures the improved response and sensitivity of the solid–liquid TENGs. In this stage, we consider the capability to harvest ambient mechanical motion energy based on liquid–solid triboelectrification at a water–solid interface and analyze these characteristics. The device could be designed as a self-powered amplitude sensor with better sensitivity and larger linear sensing range, against the air humidity. The device is driven by airflow also could be designed as a dynamic pressure sensor and flow rate sensor. Thus, the as-designed MAT-TENG can be used as both energy collector as well as self-powered sensors in developing its applicability.

The rest of the paper is organized as follows: The overview of the fabrication details of the TENG tube is introduced in Sect. 2. Section 3 gives total insight into the working principle of MAT-TENG and discussed experimental results carried out to demonstrate the potential application of the TENG as self-powered sensing system. The last section offers some brief conclusions and ideas for extending the research.

2 Experimental Section

2.1 Structure of the MAT-TENG

The structure of the proposed MAT-TENG consists of a PTFE tube with Cu electrodes wrapped outside as illustrated in Fig. 1. PTFE tube (with a wall thickness of 1 mm and an inner diameter of 4 mm) was selected due to the appropriate polarity and transparency properties of this material. As well, two identical Cu tapes (which have 50 μm thickness and 10 mm width) were attached at both ends of the PTFE tube with a gap length of 100 mm. Finally, the PTFE tube was filled up with DI water until the water volume partially covered both Cu electrodes, as seen in Fig. 1a. The
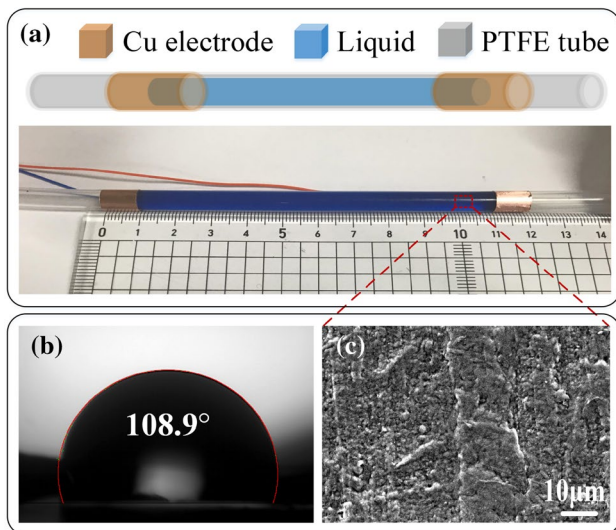
Fig. 1 Structure design and working mechanism of the TENG tube, **a** Schematic illustration of the functional components of the TENG tube, **b** The contact angle and **c** the FE-SEM image of the inner wall of the PTFE tube

MAT-TENG was then driven by a rotary actuator, which served as an oscillator.

The contact angle, shown in Fig. 1b, was measured up to 108.9^0, which obviously ensure the hydrophobicity the PTFE tube. This property allows the polar liquid such as water to flow without leaving any residual fraction behind. Figure 1c shows the field-emission scanning electron microscope (FE-SEM) image of the PTFE surface roughness. The microstructure of the proposed TENG increases its surface charge density due to the increment of the surface area; thus it is useful to enhance the triboelectric effect so as to improve the performance of MAT-TENG.

2.2 Experimental setup of the MAT-TENG

Experiments were conducted to evaluate the electrical output performance of the MAT-TENG. Figure 2a depicts the experimental setup including an oscillator, which composed by a DC motor (DS4572-IG42GM) with variable frequency drive controller and a rotary actuator (SMC-MSQ20A), to move the water volume back and forth inside the tube. The derived electricity from TENG was measured by a digital multimeter (Keithley Instruments DMM7510) and low-noise current amplifier (Stanford Research Systems SR570), respectively.

In the first case, the output performance of the MAT-TENG was considered at different displacement amplitudes of the water column. When the oscillator operated steadily at a certain frequency of 1 Hz, the angle of the rotary actuator varied by applying the crank-rocker four-bar linkage mechanism where the linkage a can be adjusted from 165 to
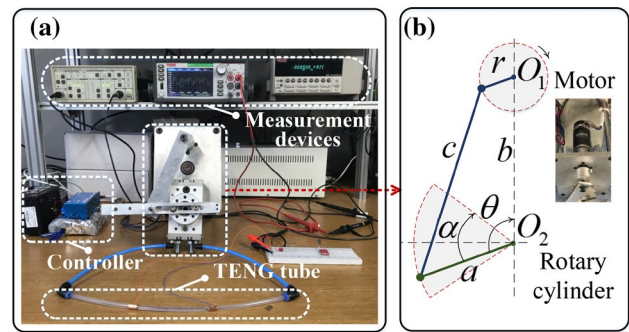

Fig. 2 Schematics of the MAT-TENG, **a** Experimental apparatus, **b** Working mechanism for the MAT-TENG tube (b = 140 mm, c = 150 mm, r = 5 mm)

60 mm, as shown in Fig. 2b. This leads to the change of the inner volume of the rotary actuator so as create an airflow, which makes the water volume inside the TENG tube also shift according to Eq. (1) and Eq. (2).

In subsequent experimental cases, the oscillator operated under different frequencies, where the length of all bar linkages was fixed. When the frequency of the oscillator was set to vary from 0.2 to 1 Hz, the internal volume of the rotary actuator changed, respectively, causing the water volume inside the TENG also slide back and forth.

The angular amplitude equation can be calculated as

$$\alpha = |\theta_{max} - \theta_{min}| \tag{1}$$

$$\text{where} \begin{cases} \theta_{max} = \cos^{-1}\left(\dfrac{a^2 + b^2 - (c + r)^2}{2ab}\right) \\ \theta_{min} = \cos^{-1}\left(\dfrac{a^2 + b^2 - (c - r)^2}{2ab}\right) \end{cases}$$

According to the manufacturing design [34], the rotary actuator has ratio $\lambda = 71.05$ (mm³/deg) corresponding with an inner volume $V = 13{,}500$ mm³ in the rotation range 190^0. Thus, the relationship between the angular rotary and the position of the liquid column can be written

$$L = \frac{4\lambda}{\pi\phi^2}\alpha \tag{2}$$

where L is the length of motion amplitude of the liquid column, $\varnothing$ is the inner diameter of the PTFE tube.

2.3 The Working Principle of the MAT-TENG

The working mechanism of the MAT-TENG is developed based on the lateral in-plane sliding between water volume and the inner surface of the TENG in a horizontal direction, as illustrated in Fig. 3.

The water volume slides back and forth inside the PTFE tube due to the internal pressure difference of the rotary
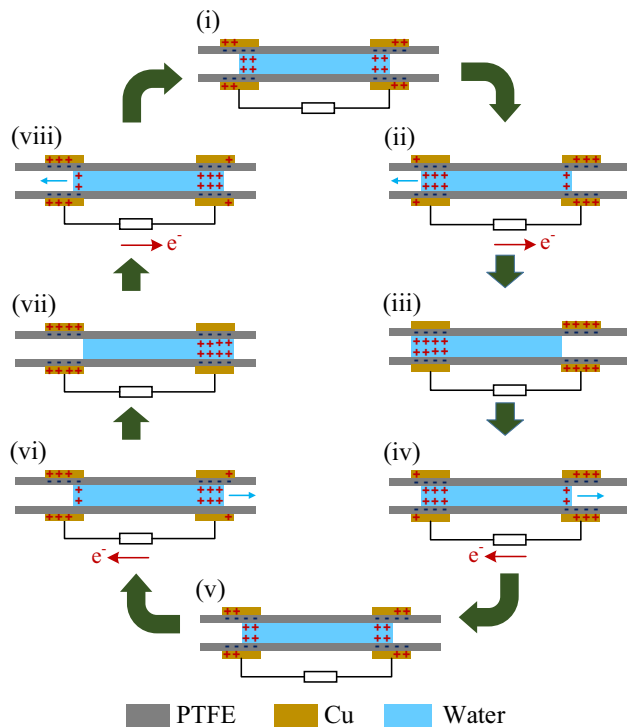
Fig. 3 The working principle of the MAT-TENG tube

actuator, which helps the MAT-TENG convert the mechanical energy into electric energy. In previous works, it has been demonstrated that the liquid-based TENGs could be activated in several operation modes, such as contact-separate mode [27] and the rotation mode [33] and so on.

As mentioned, the typical solid material is replaced by water, which serves as an in-plane sliding triboelectric layer while the PTFE tube is selected as another the solid tribo-layer material due to its high electronegativity. The working principle of the proposed MAT-TENG is schematically illustrated in Fig. 3. The corresponding position of DI water in the MAT-TENG within one complete cycle is described in Fig. 4.

Firstly, the water is preliminarily charged by means of the triboelectric effect when passing through the PTFE tube. Meanwhile, due to the difference in electron affinities, the PTFE tube becomes negatively charged while copper electrodes turn into positively charged. At initial position [Fig. 3(i)], DI water column is staying inside covering the half-length of the Cu electrodes at both ends, then the electric potential between the two electrodes is balanced. When the water column starts to move as shown in Fig. 3(ii), the contact surface area at the left electrode increases and the decrease of the contact surface area at the right electrode due to the positively charged water shifts from the neutral to the left, potential
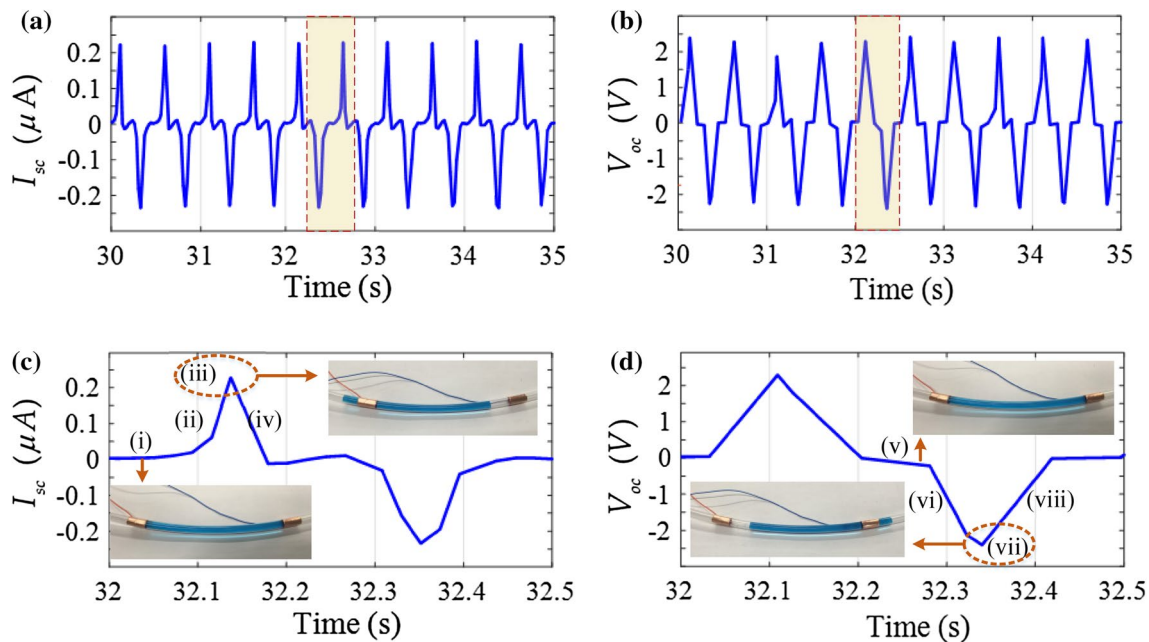

Fig. 4 The output performance of MAT-TENG with motion frequency of 1 Hz and the length of the motion amplitude of 23 mm, **a** Short-circuit current (I_{SC}), **b** Open-circuit voltage (V_{OC}), **c**, **d** The enlarged waveform in a single cycle when the motion state of liquid is from right left. Inset shows the real images

difference between the two electrodes drive the electrons to

flow from the left to the right through an external load to form an instantaneous current. The potential difference between two electrodes remains until the water column completely sliding out of the right electrode [Fig. 3(iii)], so an equilibrium state establishes according to the full breakdown of the potential difference. Then the water is slid backward to be in the reverted position [Fig. 3(iv)], water shifts to the right until it reaches the equilibrium position [Fig. 3(v)].

In much the same way, the linear mechanical motor turns at the half of the extant cycle, lead to the increase in the contact surface area at the right electrode and the decrease of the contact surface area at the left electrode, which induces the asymmetric screening of charge water at the right electrode. Consequently, the electrons shift from the right to left through the external load as shown in Fig. 3(v–vii), and then shift from the left to right again because of the water slides back direction [Fig. 3(vii–i)] to complete a motion cycle.

3 Results and Discussion

Figure 4 presents the output performance of the MAT-TENG, which is operated at a rotational frequency of 1 Hz. The water column oscillated symmetrically with the amplitudes of 23 mm, so an alternating current and voltage peaks were detected. Figure 4c, d explain the correspondence between the position of water inside the tube and output current and voltage signals in one cycle. As shown in Fig. 4a, b, short-circuit current (I_{SC}) and open-circuit voltage (V_{OC}) can reach up to 0.23 μA and 2.31 V, respectively. Generally, in one cycle, the generated electricity could also be divided into eight sections. In Fig. 4c, section (i) shows the initial state where both of the water level difference and electrical potential difference are neutral. Section (iii) describes the asymmetric accumulation of water on the left side to the outermost point, resulting in the maximum I_{SC}, and also the positive up-peak of V_{OC}, as shown in Fig. 4d. Subsequently, when the water in the tube passes through the center of copper electrodes again, then asymmetrically accumulates on the right side, resulting in an opposite electron flow; so the I_{SC} is in reverse direction negative peak of V_{OC} is found as well.

We assume the tribo-charges are uniformly distributed on liquid and solid surfaces. The transferred charges approximately equal to the tribo-charges and can be given by [35]:

$$Q_{sc} = 2\pi\phi L\sigma \tag{3}$$

where σ is the surface tribo-charges density, $\varnothing$ is the diameter of a tube, Q_{SC} is the short-circuit transferred charges, L is the length of the motion amplitude. From this equation, the short circuit current is given by

$$I_{SC} = \frac{dQ_{SC}}{dt} = \frac{dQ_{SC}}{dL}\frac{dL}{dt} = \frac{dQ_{SC}}{dL}v(t) \tag{4}$$

where t is the time, v is the velocity of the liquid column. For uniform motion, the amplitude of the short circuit current can be given as

$$I_{SC-peak} = \left(\frac{dQ_{SC}}{dL}\right)_{peak} v \tag{5}$$

Integrating Eq. (3) and Eq. (4) into Eq. (5), the short circuit current can be calculated by

$$I_{SC-peak} = 2\pi\phi\sigma v \tag{6}$$

To evaluate the energy harvesting function of the proposed TENG, the performance test under different load resistances was conducted, as shown in Fig. 5a. Obviously, with the increment of the resistance, the maximum voltage is correspondingly increased and saturates at a certain point. Simultaneously, the current peak shows an opposite tendency. The resistance is set to vary from 0.1 MΩ to 1 GΩ, resulting in the open-circuit voltages increase from 0.5 V to 2.3 V while the short-circuit current decreases from 0.24 to 0.05 μA. Figure 5b exhibits the power generated by the combination of MAT-TENG under different load resistances. The maximum power of each configuration is approximately 0.6 μW, 1.05 μW and 1.4 μW for 1-TENG model, 2-TENGs model and 3-TENGs model, respectively.

In the first experiment, we study the relationship between the output performance of the MAT-TENG with various lengths of the motion amplitude from 11 to 23 mm at the oscillating frequency of 1 Hz. As shown in Fig. 5c, d, the I_{SC} and V_{OC} increase monotonically corresponding to the length of motion amplitude of the water column, which is in accordance with the previous result [36], as the voltage is expressed in the form of the line integral of an electric field along the path. Similarly, the peaks of I_{SC}, V_{OC} and Q_{SC} between the two electrodes increases, respectively as the displacement amplitude becomes larger as sketched in Fig. 5e, f. All peaks of the measured I_{SC}, V_{OC} and Q_{SC} have expressed linearity with the length of motion amplitude, which could be linearly fitted with the correlation coefficient of 0.9982, 0.9952 and 0.9938, respectively. Based on the linear relationship between the electrical output and the length of motion amplitude, the MAT-TENG could potentially be designed as a self-powered displacement sensor.

In the second experiment, the electrical outputs of the MAT-TENG with variable frequency from 0.2 to 1 Hz at the fixed length of the motion amplitude were analyzed. The I_{SC} gradually enlarges the amplitude with the motion frequency as shown in Fig. 6a This is because the current is expressed as the line integral of an electric field along the path. Similarly, the voltage also expands monotonically with the frequency as described in Fig. 6b. Likewise, the peaks of I_{SC}, V_{OC} and Q_{SC} increase as sketched in Fig. 6c, d. All three of the measurement displays linear relationships
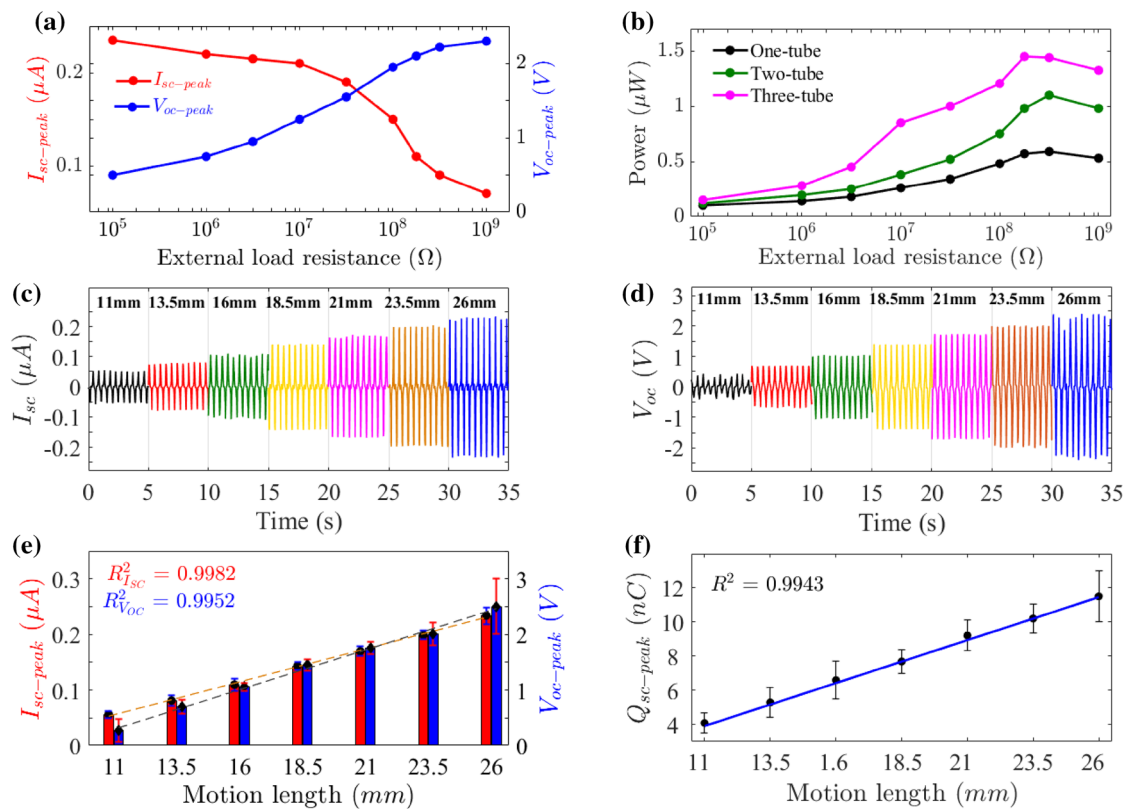
Fig. 5 Experimental results of the MAT-TENG under different condition. Impact of, **a** different resistors and **b** the MAT-TENG power output performance with increasing numbers of the tubes at a certain oscillation of 1 Hz and the motion length of 26 mm, **c** Short-circuit current, **d** Open-circuit voltage, and **e** Peaks of current and voltage, respectively, **f** Peak transferred charge with various lengths of the motion amplitude from 11 mm to 23 mm at the resonance frequency of 1 Hz

with the motion frequency, which can be linearly fitted with the correlation coefficient of 0.9887, 0.9905 and 0.9825, respectively.

Moreover, further experiments were done to observe the current output against the increasing motion frequency with several length amplitudes, as shown in Fig. 6e, all three cases $L = 16$ mm, 21 mm and 26 mm, the output values of the measured current, voltage and transferred charge display regular increment with the motion frequency. From the above experiments, the speed gradient of the water column changes linearly, the maximum velocity corresponding to the length amplitude as well as each frequency. It means that the average peak value of the I_{SC} is linearly dependent on the velocity. The bigger the velocity is, the more the kinetic energy is produced and thus more triboelectric charges will be generated on the PTFE tube surface. The approximately linear relationship between the amplitude of the short-circuit current and the velocity of the liquid column is exhibited in Fig. 6f, from which sensitivity can be achieved with good linearity $R^2 = 0.9918$. The induced current increases as the velocity increases from 3.2 to 26 mm/s. This can be applied to detect the velocity of a delicate mechanical structure whereas higher sensitivity is required and calculation of

space–time becomes difficult to determine certain parameters. Accordingly, this new MAT-TENG has also several unique advantages. This extremely simple design of TENG utilizes the triboelectrification at the liquid–solid interface, which is immune to humidity. As a new type of liquid-based TENG and TENG based active sensors, this device is able to serve as a monitoring sensor and the energy harvester at the same time.

4 Conclusions

In this paper, we demonstrated the mechanical active transducing element to develop the potential solid–liquid TENG as a self-powered sensor by using a small volume of water and solid PTFE tube. An actuating device coupled with different mechanical components were developed to grab the energy and utilize it to observe the compatibility of the MAT-TENG for future integration possibilities with the types of machinery where experiments are done under controllable situations. The hydrophobic feature of the MAT-TENG facilitates the liquid to move without leaving any residual that ensures the stable output of the MAT-TENG
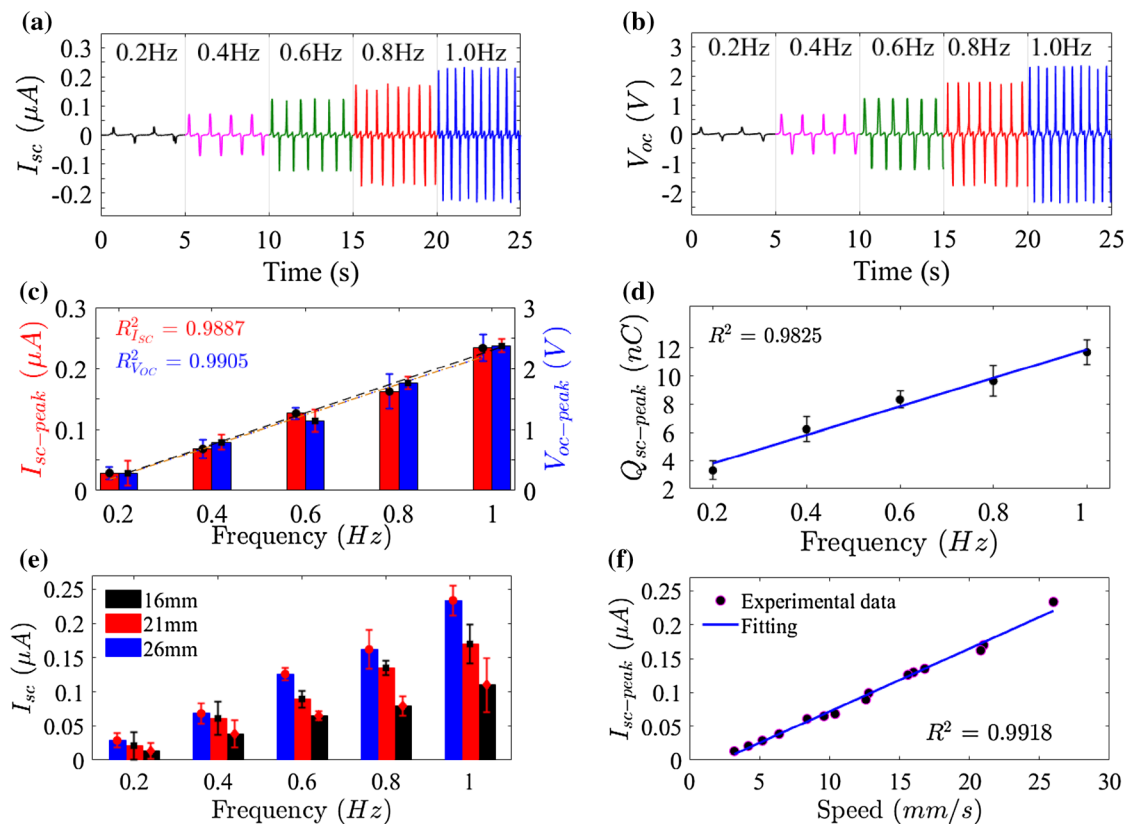
Fig. 6 Output performance of the MAT-TENG at a variable frequency from 0.2 to 1 Hz. **a** Short-circuit current, **b** Open-circuit voltage, **c**, **d** Relationships between the peaks of output performance (I_{SC}, Q_{SC}, V_{OC}) with varying frequency, and **e** Responding the peak of I_{SC} and **f** Speed gradient of the water column when the changing length amplitude of 16 mm, 21 mm and 26 mm at variable frequency from 0.2 to 1 Hz, respectively

and shows the effectiveness of sensing. A mathematical relationship was developed to quantify the current generation with respect to the motion amplitude. The sensitivity of the fabricated TENG was analyzed to its response to the controllable velocity magnitude. The experimental results validated that the TENG was sensitive to motion and it can clearly differentiate between contacts at different velocities in the ranges from 3.2 to 26 mm/s, respectively. Our developed MAT-TENG is expected to compete with other the expensive sensors and monitoring device in terms of convenient approach and easy viability. The proposed MAT-TENG can be utilized efficiently in industrial sectors with the development of compact structure and integration capability.

For the future plan, authors intend to develop this MAT-TENG as a multifunctional sensor (such as flowrate sensor and pressure sensor) with the complementary mechanisms based on liquid–solid triboelectrification. In addition, this MAT-TENG can be utilized with various liquids as a multiplex liquid sensor to detect liquid types and impurities in liquids industries.

References

1. Choi, Y. W., Jang, S., Chun, M.-S., Kim, S. M., & Choi, M. (2018). Efficient microfluidic power generator based on interaction between DI water and hydrophobic-channel surface. *International Journal of Precision Engineering and Manufacturing-Green Technology, 5,* 255–260.
2. Shi, M., et al. (2016). Self-powered analogue smart skin. *ACS Nano, 10,* 4083–4091.
3. Wang, Z. L., Chen, J., & Lin, L. (2015). Progress in triboelectric nanogenerators as a new energy technology and self-powered sensors. *Energy & Environmental Science, 8,* 2250–2282.
4. Yi, F., et al. (2014). Self-powered trajectory, velocity, and acceleration tracking of a moving object/body using a triboelectric sensor. *Advanced Functional Materials, 24,* 7488–7494.
5. Zhang, H., et al. (2014). Triboelectric nanogenerator for harvesting vibration energy in full space and as self-powered acceleration sensor. *Advanced Functional Materials, 24,* 1401–1407.

6. Lee, K. Y., et al. (2016). Fully packaged self-powered triboelectric pressure sensor using hemispheres-array. *Advanced Energy Materials., 6,* 1502566.

7. Wu, Z., et al. (2018). Self-powered multifunctional motion sensor enabled by magnetic-regulated triboelectric nanogenerator. *ACS Nano, 12,* 5726–5733.

8. Li, T., et al. (2016). Lightweight triboelectric nanogenerator for energy harvesting and sensing tiny mechanical motion. *Advanced Functional Materials, 26,* 4370–4376.

9. Fan, F.-R., Tian, Z.-Q., & Lin Wang, Z. (2012). Flexible triboelectric generator. *Nano Energy, 1,* 328–334.

10. Kim, J. E., Kim, H., Yoon, H., Kim, Y. Y., & Youn, B. D. (2015). An Energy conversion model for cantilevered piezoelectric vibration energy harvesters using only measurable parameters. *International Journal of Precision Engineering and Manufacturing-Green Technology, 2,* 51–57.

11. Yang, W., et al. (2014). 3D stack integrated triboelectric nanogenerator for harvesting vibration energy. *Advanced Functional Materials, 24,* 4090–4096.

12. Zhu, G., et al. (2014). Self-powered, ultrasensitive, flexible tactile sensors based on contact electrification. *Nano Letters, 14,* 3208–3213.

13. Yang, Y., et al. (2013). Human skin based triboelectric nanogenerators for harvesting biomechanical energy and as self-powered active tactile sensor system. *ACS Nano, 7,* 9213–9222.

14. Pu, X., et al. (2017). Eye motion triggered self-powered mechnosensational communication system using triboelectric nanogenerator. *Science Advances, 3,* e1700694.

15. Wang, Z. L. (2013). Triboelectric nanogenerators as new energy technology for self-powered systems and as active mechanical and chemical sensors. *ACS Nano, 7,* 9533–9557.

16. Wang, S., Lin, L., & Wang, Z. L. (2015). Triboelectric nanogenerators as self-powered active sensors. *Nano Energy, 11,* 436–462.

17. Chen, J., & Wang, Z. L. (2017). Reviving vibration energy harvesting and self-powered sensing by a triboelectric nanogenerator. *Joule, 1,* 480–521.

18. Shen, J., Li, Z., Yu, J., & Ding, B. (2017). Humidity-resisting triboelectric nanogenerator for high performance biomechanical energy harvesting. *Nano Energy, 40,* 282–288.

19. Li, S., et al. (2017). Sustainable energy source for wearable electronics based on multilayer elastomeric triboelectric nanogenerators. *Advanced Energy Materials, 7,* 1602832.

20. He, C., et al. (2017). Hourglass triboelectric nanogenerator as a "direct current" power source. *Advanced Energy Materials, 7,* 1700644.

21. Wang, A. C., Wu, C., Pisignano, D., Wang, Z. L., & Persano, L. (2018). Polymer nanogenerators: opportunities and challenges for large-scale applications. *Journal of Applied Polymer Science, 135,* 45674.

22. Li, Z., et al. (2016). High-efficiency ramie fiber degumming and self-powered degumming wastewater treatment using triboelectric nanogenerator. *Nano Energy, 22,* 548–557.

23. Nguyen, V., Zhu, R., & Yang, R. (2015). Environmental effects on nanogenerators. *Nano Energy, 14,* 49–61.

24. Seol, M.-L., Jeon, S.-B., Han, J.-W., & Choi, Y.-K. (2017). Ferrofluid-based triboelectric-electromagnetic hybrid generator for sensitive and sustainable vibration energy harvesting. *Nano Energy, 31,* 233–238.

25. Lin, Z.-H., Cheng, G., Lee, S., Pradel, K. C., & Wang, Z. L. (2014). Harvesting water drop energy by a sequential contact-electrification and electrostatic-induction process. *Advanced Materials, 26,* 4690–4696.

26. Tang, W., et al. (2015). Liquid-metal electrode for high-performance triboelectric nanogenerator at an instantaneous energy conversion efficiency of 70.6%. *Advanced Functional Materials, 25,* 3718–3725.

27. Lin, Z.-H., Cheng, G., Lin, L., Lee, S., & Wang, Z. L. (2013). Water–solid surface contact electrification and its use for harvesting liquid-wave energy. *Angewandte Chemie International Edition, 52,* 12545–12549.

28. Zhao, X. J., et al. (2016). Biocide-free antifouling on insulating surface by wave-driven triboelectrification-induced potential oscillation. *Advanced Materials Interfaces, 3,* 1600187.

29. Chen, J., et al. (2016). Self-Powered Triboelectric Micro Liquid/Gas Flow Sensor for Microfluidics. *ACS Nano, 10,* 8104–8112.

30. Li, X., et al. (2015). Self-powered triboelectric nanosensor for microfluidics and cavity-confined solution chemistry. *ACS Nano, 9,* 11056–11063.

31. Zhang, X., Zheng, Y., Wang, D., Rahman, Z. U., & Zhou, F. (2016). Liquid–solid contact triboelectrification and its use in self-powered nanosensor for detecting organics in water. *Nano Energy, 30,* 321–329.

32. Jeon, S.-B., Kim, D., Seol, M.-L., Park, S.-J., & Choi, Y.-K. (2015). 3-Dimensional broadband energy harvester based on internal hydrodynamic oscillation with a package structure. *Nano Energy, 17,* 82–90.

33. Kim, T., et al. (2016). Design and optimization of rotating triboelectric nanogenerator by water electrification and inertia. *Nano Energy, 27,* 340–351.

34. Steven Engineering, Inc, Low-speed rotary actuator series CRQ2X/MSQX. https://stevenengineering.com/Tech_Support/PDFs/70ARCRQ2X.pdf. Accessed 22 Dec 2018.

35. Niu, S., et al. (2013). Theory of sliding-mode triboelectric nanogenerators. *Advanced Materials, 25,* 6184–6193.

36. Wang, S., et al. (2013). Sliding-Triboelectric Nanogenerators Based on In-Plane Charge-Separation Mechanism. *Nano Letters, 13,* 2226–2233.

37. Zhang, B., et al. (2017). Self-powered acceleration sensor based on liquid metal triboelectric nanogenerator for vibration monitoring. *ACS Nano, 11,* 7440–7446.

38. Kim, W., Choi, D., Kwon, J.-Y., & Choi, D. (2018). A self-powered triboelectric microfluidic system for liquid sensing. *Journal of Materials Chemistry A, 6,* 14069–14076.

Publisher's Note Springer Nature remains neutral with regard to jurisdictional claims in published maps and institutional affiliations.

Cong Phat Vo received the B.E degrees in Electrical and Electronic Engineering Technology and the M.S. in Mechatronics Engineering from Ho Chi Minh City University of Technology and Education, Vietnam in 2013 and 2016, respectively.

He is currently pursuing the Ph.D. degree with the School of Mechanical Engineering, University of Ulsan, Ulsan, Korea. His research interests include robotics, nonlinear control, and renewable energy.

M. Shahriar received his B. Sc degree from Chittagong University of Engineering and Technology (CUET), Bangladesh in 2017. Now he is studying towards M. Sc degree in Mechanical Engineering in University of Ulsan (UOU), South Korea. His current research interests are nanoenergy harvesting, green technology, development of biocompatible thin film, microfluidics system for smart sensing applications and fluid-structure interaction diagnosis.

Chau Duy Le received the B.S degree in power systems from Ho Chi Minh University of Technology, Vietnam, in 2013. He is currently working toward the Ph.D. degree in renewable energy at the School of Mechanical Engineering, University of Ulsan, Republic of Korea.

His current research interests include renewable energy systems and energy management.

Kyoung Kwan Ahn (SM'19) received the B.S. degree in the Department of Mechanical Engineering from Seoul National University in 1990, the M. Sc. degree in Mechanical Engineering from Korea Advanced Institute of Science and Technology in 1992 and the Ph.D. degree from Tokyo Institute of Technology in 1999.

He is currently a Professor in the School of Mechanical Engineering, University of Ulsan, Ulsan, Korea. His research interests are design and control of smart actuator using the smart material, fluid power control and active damping control, renewable energy. He is an Editor of IJCAS, an Editorial Board of Renewable Energy, Actuators and Journal of Engineering.